

Enzymatic Ring-Opening Polymerization of ϵ -Caprolactone by a New Lipase from *Yarrowia lipolytica*

Karla A. Barrera-Rivera,¹ Arturo Flores-Carreón,^{1,2} Antonio Martínez-Richa¹

¹Facultad de Química, Universidad de Guanajuato, Noria alta s/n, Guanajuato, Gto. 36050, México

²Instituto de Investigación en Biología Experimental, Facultad de Química, Universidad de Guanajuato, Noria alta s/n, Guanajuato, Gto. 36050, México

Received 5 July 2007; accepted 6 November 2007

DOI 10.1002/app.28116

Published online 2 April 2008 in Wiley InterScience (www.interscience.wiley.com).

ABSTRACT: A new lipase from the yeast *Yarrowia lipolytica* was isolated and used in the enzymatic ring-opening polymerization of lactones. The effect of used commercial oil from a vacuum pump (instead of olive oil) and in the presence of wheat flour was evaluated. It was found that lipase production is favored when wheat flour and used commercial oil is added instead of olive oil with an incubation time of 16.5 h at 29°C and 250 rpm. Lipase shows a specific activity of 3.47 nmoles of 4-methyl umbelliferone released/mg of protein/min. In this way, preculture step can be avoided and an important reduction in production time can be obtained. *In vitro* polymerization of ϵ -caprolactone at different temperatures in the presence of *n*-heptane

for 15 days produces low-molecular-weight polyesters with unique multiphase morphology. Polyesters were characterized by NMR (solution and solid-state) spectroscopy, differential scanning calorimetry (DSC), Fourier-transformed infrared, wide-angle X-ray scattering and MALDI-TOF. Polyester crystallinities calculated by DSC were high, as expected for low-molecular-weight PCLs. Final polymer possesses carboxylic acid and hydroxyl end-groups, as determined by ¹H- and ¹³C NMR analysis. © 2008 Wiley Periodicals, Inc. *J Appl Polym Sci* 109: 708–719, 2008

Key words: enzymatic polymerization; polyesters; lipases; *Yarrowia lipolytica*

INTRODUCTION

Polymerization reactions catalyzed by enzymes proceed through quimioselective, regiospecific, and stereoselective pathways. Enzymes represent a diverse family of natural catalysts that carry out a wide range of organic transformations. Lipases are one of the most versatile biocatalysts that bring about a range of bioconversion reactions. They catalyze chemical reactions under extremely mild conditions with or without the presence of organic solvents.¹

Lipases (triacylglycerol acylhydrolases, E.C. 3.1.1.3) are ubiquitous enzymes of considerable physiological significance and industrial potentiality. Lipases catalyze the hydrolysis of triacylglycerols to glycerol and free fatty acids.² In contrast to esterases, lipases are activated only when adsorbed to an oil–water

interface,³ and do not hydrolyze dissolved substrates in the bulk fluid. A true lipase will split emulsified esters of glycerin and long-chain fatty acids as triolein and tripalmitin. Lipases are serine hydrolases.²

Yarrowia lipolytica is a yeast species widely used in industrial applications. Strains of this yeast secrete a set of proteins (alkaline or acid proteases, lipases) that can be isolated from the production culture medium.⁴ *Y. lipolytica* is a natural dimorphic fungus, which forms yeast cells, pseudohyphae, and septate hyphae; this fungus is not considered as a pathogenic species, probably because of its maximum growth temperature, which seldom exceeds 32–34°C.

Y. lipolytica strains display a lipase activity that acts preferentially on oleyl residues at positions 1 and 3 of the glyceride.⁵ Lipase activities have been examined by different investigators on different strains. It is likely that reported activities differ due to methodologies used, and/or the existence of different types of strains.⁶

First reports to produce polyesters by ring-opening polymerization (ROP) using biocatalysis by lipases were made by Knani⁷ and Uyama and Kobayashi.⁸ Since then, lipases from different origins have been tested as biocatalysts for ROP. Employing enzymes in organic synthesis has several advantages such as (i) catalysis proceeds under mild reaction conditions

Correspondence to: A. Martínez-Richa (richa@quijote.ugto.mx).

Contract grant sponsor: Consejo Nacional de Ciencia y Tecnología (CONACYT); contract grant number: SEP-2004-C01-47173E.

Contract grant sponsor: Consejo de Ciencia y Tecnología del Estado de Guanajuato (CONCYTEG).

Contract grant sponsor: Universidad de Guanajuato.

(as low temperatures and pressures are required) which often lead to a remarkable energy efficiency; (ii) high enantio-, regio-, and chemoselectivities as well as regulation of stereochemistry are achieved, providing development of new reactions to functional compounds for pharmaceuticals and agrochemicals; (iii) nontoxic natural catalyst with "green" appeal in commercial benefit and ecological requirement. Enzyme catalysis has provided a new synthetic strategy for useful polymers, most of which are otherwise very difficult to produce by conventional chemical catalysts.⁹

In vitro enzymatic syntheses via nonbiosynthetic pathways, therefore, are recognized as a new area of precision polymer synthesis. Furthermore, the enzymatic polymerizations may greatly contribute to global sustainability without depletion of important resources by using nonpetrochemical renewable resources as starting substrates of polymeric materials. In the enzymatic polymerizations, the production of polymers can be made under mild reaction conditions without using toxic reagents. Therefore, the enzymatic polymerization can be regarded as an environmentally friendly synthetic process of polymeric materials, providing a good example of "green polymer chemistry."⁹

Lipase-catalyzed reactions are considered to proceed via an acyl-enzyme intermediate. Catalytic site of lipase is known to be a serine-residue. For polymerizations, the key step is the reaction of lactone with lipase that provokes the ring-opening of the lactone to give an acyl-enzyme intermediate (enzyme-activated monomer, EM). The initiation step involves a nucleophilic attack of water, which is probably contained in the enzyme, onto the acyl carbon of the intermediate to produce an ω -hydroxycarboxylic acid ($n = 1$); the shortest propagating species. In the propagation stage, the intermediate is nucleophilically attacked by the terminal hydroxyl group of a propagating polymer to produce a one-unit-more

elongated polymer chain (Scheme 1). The kinetics of the polymerization showed that the rate-determining step of the over-all polymerization is the formation of the enzyme-activated monomer. Therefore, the polymerization probably proceeds via an "activated-monomer mechanism."¹⁰

Enzyme catalysis offers several advantages over chemical catalysis. The benefits of enzyme-catalyzed polymerization can be summarized as follows: (a) Enzymes are derived from renewable resources, so they are recyclable, ecofriendly nontoxic materials. Therefore, the need for their complete removal from the polymers is not that stringent. (b) Polymers with well-defined structures may be formed by enzyme-catalyzed process. (c) Lipases do not require the exclusion of water and air when used as catalysts for polyester synthesis. This is in contrast to traditional chemical initiators where strict precautions are to be taken to exclude air or water from the system. (d) Small (4–7-membered) cyclic lactones are easily polymerized by organometallic initiators. However, polymerization of large ring lactones (macrolides) is slow, and only low-molecular-weight products are obtained. Similarly, unstrained γ -butyrolactone could not be polymerized using aluminoxane initiators but it could be polymerized by using enzymes.¹¹

In this work, the ROP of ϵ -caprolactone by *Y. lipolytica* lipase was investigated for the first time. The effects of lipase concentration (25–100 mg) and temperature (50–70°C) were evaluated. Results indicate that polyesters with multiphase morphology were obtained. To our knowledge, this is the first report in the literature on low-molecular-weight PCLs with multiphase morphology.

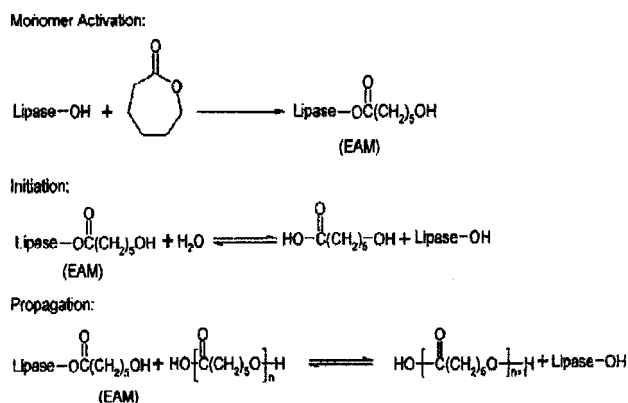
EXPERIMENTAL

Materials

ϵ -CL (Aldrich Chemicals Co., Mexico) was dried over calcium hydride and distilled under reduced pressure before use. *n*-Heptane (productos químicos Monterrey), chloroform (Karl, León, Mexico), and methanol (Fermont, Monterrey, Mexico) were used as received. Porcine pancreatic lipase type II (25% of protein with $a^* = 75$ U/mg of protein), bovine albumin Grade V (98%), 4-methylumbelliferyl-oleate (MUO), 4-methylumbelliferyl-palmitate (MUP), olive oil, malt extract, CaCO_3 , MgSO_4 , K_2HPO_4 , urea, soybean meal, glucose, wheat flour, $(\text{NH}_4)_2\text{SO}_4$, and corn steep liquor (CSL) were purchased from Sigma-Aldrich and used as received.

Organism

Y. lipolytica strain was used in this study. It was maintained on slants of solid YPG medium (0.3%



Scheme 1 Mechanism for lipase-catalyzed ROP of lactones.

yeast extract, 1% peptone, 2% glucose, and 2% agar, pH 6.3) as previously described by Bartnicki-García and Nickerson.¹²

Protein determination

Protein was measured by the method of Bradford using bovine serum albumin as standard.¹³

Enzyme production and characterization

The preculture (50 mL) of *Y. lipolytica* was obtained in a 250-mL Erlenmeyer flask incubated at 29°C on a rotary shaker (250 rpm) for 16 h in medium containing: glucose 2%, yeast extract 1%, and peptone 1%. The inoculum culture was performed under the same conditions, except for the medium (pH = 7) which contains: malt extract 3%, CaCO₃ 0.4%, MgSO₄ 0.1%, K₂HPO₄ 0.2%, urea 0.1%, soybean meal 0.5%, olive oil 0.5% (v/v). The inoculum represented 5% (v/v) of the culture.

Enzyme production was carried out for 27 h at 29°C in a modified medium (regulated at pH 7)¹⁴: glucose 1%, wheat flour 3%, CSL 1% (v/v), olive oil 0.5% (v/v), (NH₄)₂SO₄ 0.8%. Cells were removed by three repeated centrifugations at 5000 rpm for 30 min each, and the supernatant was saved and activity was measured using MUP as assay,¹⁵ briefly: a 10 mM stock solution of 4MUP in dry 2-methoxyethanol and stored at 4°C. Immediately before use, the stock solution was dissolved in 50 mM phosphate buffer pH 7.0 to prepare 50 mM buffered substrate. In the standard assay, 25 µL of the supernatant was incubated for 30 min at 37°C with 20 µL of 50 mM buffered substrate and 155 µL of 50 mM phosphate buffer pH 7.0 containing 5 mM CaCl₂ in a water bath. The reaction was stopped by adding 3 mL 50 mM Tris-HCl buffer pH 8.0 containing 5 mM ethylene diamine tetra acetic acid. The 4-methylumbelliferone liberated from the substrate from hydrolysis was read on a PERKIN-ELMER LS-5B fluorescence spectrophotometer at 365 nm for the excitor and at 450 nm for the emission. 4-Methylumbelliferone was run as a standard solution; one unit of activity corresponds to the hydrolysis of 1 µmol substrate/min at 37°C.

The supernatant was lyophilized and kept at -20°C until it was used in the polymerization of ε-CL.

Electrophoresis

Sodium dodecyl sulfate-polyacrylamide electrophoresis (SDS-PAGE) and native (PAGE) conditions were carried out in 12 and 7% gels, respectively, following standard protocols Laemmli,¹⁶ and proteins were stained with Coomassie blue and silver according to Merril.¹⁷ For zymograms, native gel was washed three times with 50 mM pH 7.0 phosphate

buffer for 15 min at room temperature, immersed in a substrate solution containing 40 µM MUO and incubated at 37°C for 30–60 min, the gel was inspected under UV illumination, and the image was captured in a Stratagene Model Eagle II gel analyzer.

Synthesis of poly (ε-caprolactone) using *Y. lipolytica* lipase and crude porcine pancreatic lipase

Polymerizations were carried out in 10-mL vials previously dried and purged with dry nitrogen. In a typical run, monomer (ε-CL, 3 mmol), catalyst (enzyme, 100 mg) and *n*-heptane (750 µL) were added under dry nitrogen atmosphere. Vials were stoppered with a rubber septum and placed in a thermostated bath at predetermined temperatures (50, 55, 60, 65, and 70°C) and time periods (48, 72, 120, 168, 216, 264, 312, 336, and 360 h). Final polymer was crystallized from chloroform/methanol, separated from the insoluble enzyme by filtration through 10- to 15-µm glass-fritted filters and dried under vacuum. Molecular weights and conversions during reaction were monitored by ¹H NMR. The crystallized polymer was analyzed by FTIR, MALDI-TOF, differential scanning calorimetry (DSC), WAXS, solution (proton and carbon-13) and solid-state-NMR.

Measurements

Solution ¹H and ¹³C NMR spectra were recorded at room temperature on a Varian Gemini 200 (200 MHz). Chloroform-*d* (CDCl₃) and acetonitrile-*d*₃ (CD₃CN) were used as solvents. Spectra were referenced to the residual solvent protons at δ 7.26 and 1.94 for CDCl₃ and CD₃CN, respectively, in the ¹H NMR spectrum, and the residual solvent protons at δ 77.0 and 1.39 for CDCl₃ and CD₃CN, respectively, in the ¹³C NMR spectrum. For ¹H-¹H COSY experiments, a standard pulse sequence was used. The spectra were acquired with 512 data points and 128 increments, with eight transients per increment. The relaxation delay was 1 s. Sinebell weighting function was used before Fourier transformation in both dimensions. Degree of polymerization and monomer conversion were determined by ¹H NMR from the relative peak areas of signals corresponding to the ester methylene of the polymer (t, δ = 4.04 ppm -CH₂OCO-), the ester methylene of the monomer (t, δ = 2.6 ppm -CH₂COO-), and the chain terminal methylene groups (t, δ = 3.6 ppm -CH₂OH).

Solid state ¹³C NMR spectra were recorded under proton decoupling on Varian Unity Plus 300 spectrometer. Approximately 100 mg were packed into 7-mm diameter zirconium rotors, with Kel-F packs. CP-MAS spectra were obtained under Hartmann-Hahn matching conditions and a spinning rate of 4.5

kHz was used. A contact time of 1 ms and a repetition time of 4 s were used. The measurements were made using spin-lock power in radiofrequency units of 60 kHz and typically 4000 transients were recorded. For MAS spectra, a repetition time of 20 s was used. Chemical shifts were referenced to the upfield peak of adamantane at 29.5 ppm with respect to TMS, as determined on a separate sample.

FTIR spectra were obtained with the ATR technique on films deposited over a selenium sulfide crystal on a Perkin–Elmer 1600 spectrometer. Spectra were digitally analyzed using Origin software.

Matrix-assisted laser desorption ionization time-of-flight (MALDI-TOF) spectra were recorded in the linear mode by using a Voyager DE-PRO time-of-flight mass spectrometer (Applied Biosystems) equipped with a nitrogen laser emitting at $\lambda = 337$ nm, with a 3-ns pulse width and working in positive-ion mode and delayed extraction. A high acceleration voltage of 20 kV was employed. 2,5-Dihydroxybenzoic acid was used as matrix. Samples were dissolved in acetonitrile and mixed with the matrix at a molar ratio of $\sim 1 : 100$.

DSC thermograms were obtained in a Mettler-Toledo 820e calorimeter using heating and cooling rates of 10 and 20°C/min. The crystallization and melting of PCL was measured using a Mettler-Toledo differential scanning calorimeter (DSC 822e) interfaced to a personal computer. The thermal response of the instrument was calibrated from the enthalpy of fusion of a known mass of indium (99.999% pure). Samples were contained in aluminum pans, and an empty pan was used as reference. Degrees of crystallinity were calculated as follows: a linear baseline was drawn from the first onset of melting to the last trace of crystallinity, and the enthalpy of fusion was then calculated from the area under the endotherm. The weight fraction degree of crystallinity (X_c) was defined as

$$X_c = \frac{\Delta H_f(T_m)}{\Delta H_f^0(T_m^0)}$$

where $\Delta H_f(T_m)$ is the enthalpy of fusion measured at the melting point and $\Delta H_f^0(T_m^0)$ is the enthalpy of fusion of a completely crystalline PCL. A literature value of 139.3 J/g for $\Delta H_f^0(T_m^0)$ was used.¹⁸

RESULTS AND DISCUSSION

Enzyme production

Some parameters to optimize the enzyme production by *Y. lipolytica* were established. It was found that enzyme production is favored when wheat flour and used commercial oil were added to the culture medium instead of whey powder and olive oil. We run

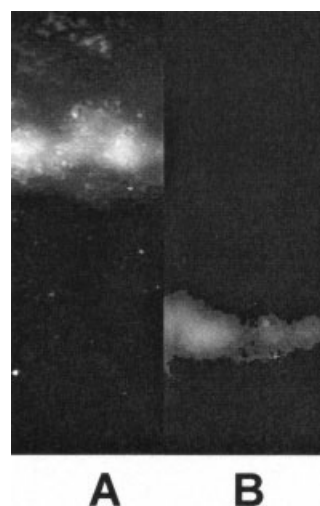


Figure 1 Analytical zymogram analysis of porcine pancreatic lipase (PPL) (A) and *Y. lipolytica* lipase (LY) (B). Native PAGE conditions 7% native gel was immersed in a revealing solution containing 40 μ M MUO and incubated at 37°C for 30 min, the gel was inspected under UV illumination.

another experiment to evaluate the production of lipase, the highest productivity of extracellular lipase was obtained in liquid medium having a preculture step, after 49 h of incubation, reached the maximum lipase production with a concentration of 0.564 mg of protein/mL and specific activity of 0.154 (nmoles of 4MU released/mg of protein/min), at 47 h 0.536 mg of protein/mL with an specific activity of 0.119, and the minimum activity was reached at 45 h 0.532 mg of protein/mL with a specific activity of 0.118. As it is reported in the literature,¹⁴ the addition of lipid materials or of soybean meal in the culture medium increases enzyme production. The effect of used commercial oil from a vacuum pump instead of olive oil and in the presence of wheat flour was evaluated. In this case, the evaluation was performed by directly inoculating the enzyme production medium with *Y. lipolytica* strain avoiding the preculture step, and the optimal production of lipase was reached when incubation time was 16.5 h at 29°C and 250 rpm, obtaining 0.615 mg of protein/mL with a specific activity of 3.47 when the culture medium contained wheat flour and used commercial oil, on the other hand 0.606 mg of protein/mL, and specific activity of 1.22 when the culture medium contained used commercial oil but not wheat flour. From these results, we adopted these conditions for faster production of lipase from *Y. lipolytica*. The supernatant containing the enzyme was analyzed by SDS-PAGE 12% and native conditions 7%. Figure 1 shows zymograms of porcine (A) and *Y. lipolytica* lipase (B) with different movilities. The fungal lipase was extracted from the native gel and analyzed by SDS-PAGE 12% showed one main protein band of

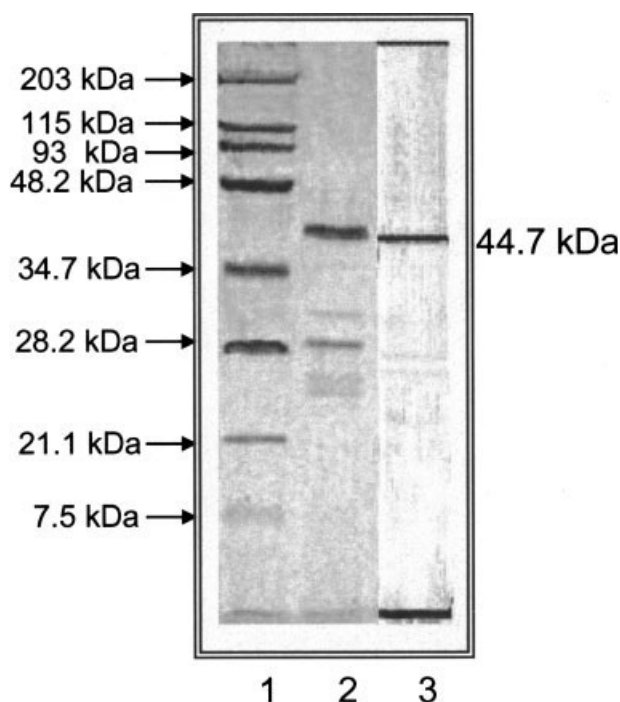


Figure 2 Analytical gel electrophoresis of lipase. Samples of 10 μg of enzyme were applied in sodium dodecyl sulfate-polyacrilamide (12%) gels. Lane (2) porcine pancreatic lipase after heat denaturation. Lane (3) *Y. lipolytica* lipase obtained by electrophoresis in native conditions. Lane (2) was stained with Coomassie blue and Lane (3) with silver. Lane (1) molecular weight markers stained with Coomassie blue.

44.7 kDa revealed by silver (Fig. 2 lane 3). Destain et al. reported previously a molecular weight of 38 kDa for one of the two cell-bound lipases from *Y. lipolytica*. Figure 2 (lane 2) shows also the protein patterns observed for crude porcine pancreatic lipase (PPL). It is evident that lipase obtained from *Y. lipolytica* is more homogenous and has higher purity. We have not demonstrated if the 44.7-kDa protein is responsible of the lipase activity. The PAGE could be a good procedure for the purification of this enzyme in one-step. Figure 2 also shows the protein pattern of crude PPL, which revealed several protein bands being the main protein band of 45 kDa besides four proteins in the range of 22–30 kDa in lesser amount. Fernandez-Lafuente et al. studied the PPL extract and developed a protocol to purify three different enzymes of lower molecular weight present in PPL, and they found that the protein of 25 kDa was responsible for a major percentage of esterase activity, even though it only accounts for less than 1% of the total protein.¹⁹

Ring-opening polymerization of ϵ -caprolactone by lipase catalysis

Uyama and Kobayashi in 1993⁸ reported that the polymerization of δ -valerolactone and ϵ -CL is catalyzed

by using lipases from *P. fluorescens*, *C. cylindracea*, and PPL. The bulk polymerization was carried out for 10 days. Lipase from *P. fluorescens* gave the highest monomer conversion (92%) and poly (ϵ -CL) of $M_n = 7700$, with carboxyl and hydroxyl end groups was obtained. Knani et al.⁷ also investigated the polymerization of ϵ -CL by using PPL. The polymerization was carried out in *n*-hexane for 624 h PPL gave a poly (ϵ -CL) of $M_n = 1924$.

Experiments were performed to determine the reaction order of monomer. The effect of incubation times in the polymerization of ϵ -CL was done and the results are shown in Figure 3. It was found that higher-molecular-weight polymers are obtained with PPL, compared to those obtained with *Y. lipolytica* lipase (LY). However 100% of monomer conversion was only obtained using latter enzyme. Based on the kinetic curves (Fig. 3), we conclude that lipases isolated from *Y. lipolytica* are efficient catalysts for the polymerization of lactones.

On the other hand, Figure 4, shows the results for the polymerization reaction of ϵ -CL carried out with 3 mmol of monomer and different amounts of *Y. lipolytica* lipase (namely 25, 50, 100, 150, and 200 mg per 3 mmol of lactone) at $60^\circ\text{C} \pm 1^\circ\text{C}$ in the presence of *n*-heptane. It can be observed that by increasing the catalyst concentration, the degree of monomer conversion and the molecular weight increased. From a series of kinetic experiments, it was determined that, by increasing enzyme–substrate concentration, higher molecular weights were attained in a relatively shorter reaction time. An opposite effect occurs when this ratio was increased from 100 to 200 mg. In this gap, the effect of the enzyme concentration over reaction time is almost null according to the molecular weight observed. As the enzyme con-

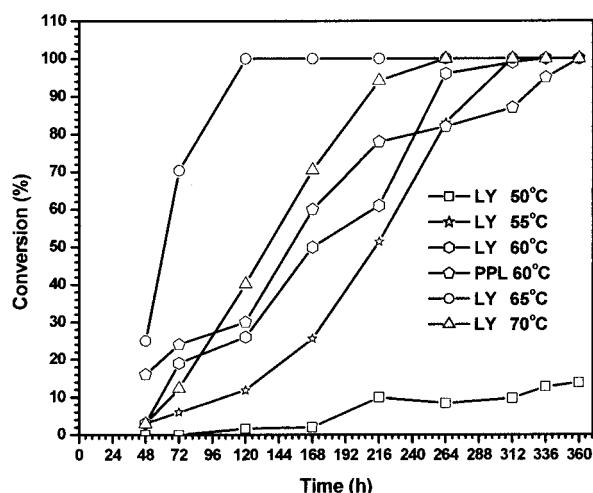


Figure 3 Effect of reaction time on monomer conversion. Polymerization in the presence of *n*-heptane. $R = 3$ mmol ϵ -CL/100 mg of lipase at 50, 55, 60, and 70°C .

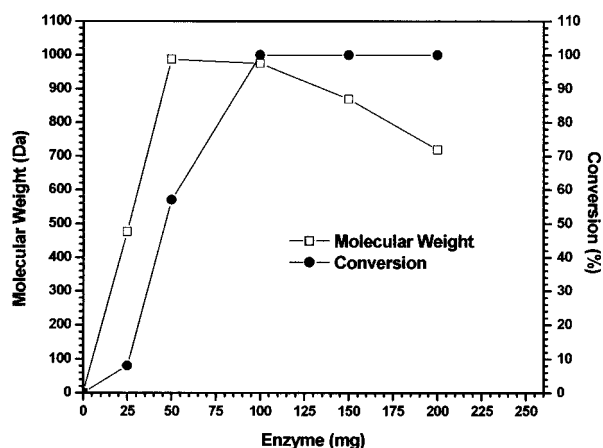


Figure 4 Effect of monomer/initiator ratio on molecular weight (M_n) and conversion of ϵ -CL, $R = 3 \text{ mmol } \epsilon\text{-CL}/x \text{ mg } Y. lipolytica \text{ lipase}$, reaction time = 360 h, $T = 60^\circ\text{C}$, polymerization in presence of n -heptane.

centration is increased, kinetic rate increases, to the point at which significant amounts of the total substrate concentration are being depleted during the time window of the assay. When substrate depletion becomes significant, further increment in enzyme concentration does not affect reaction velocity. As a result, we may observe a plot that is linear at low enzyme concentrations, but then curves over and may even show saturation effects at higher values of enzyme concentration. A higher amount of water may induce chain termination and/or backbiting reactions.

Attempts to increase the propagation rates of lipase-catalyzed polymerizations by an increase in the reaction temperature must take into account the thermal stability of the lipase. For any enzyme-catalyzed process in organic media, the solvent plays a crucial role in determining enzyme stability and regulating the partitioning of substrates and products between the solvent and the enzyme. Enzyme specificity can be altered or specifically fine-tuned by proper selection of the organic solvent. The nature of organic solvents is well known to be crucial for the

maintenance of critical water content necessary for catalytic activity. By changing the organic solvent is possible to control the substrate specificity. For enzymes in organic media their catalytic efficiency is, in most cases, lower than in aqueous systems. This behavior can be attributed to different causes, such as diffusional limitations, high saturating substrate concentrations, restricted protein flexibility, low stabilization of the enzyme–substrate intermediate, and even partial enzyme denaturation by lyophilization, which becomes irreversible in anhydrous solvents.

The temperature dependence of the polymerization rate was studied. Experiments were performed using 3 mmol of ϵ -CL by 100 mg of lipase. By raising the reaction temperature, a sharp decrease in the reaction time of the product polyesters can be observed. Results on the effect of temperature, dependence on the degree of polymerization on temperature, and the effect of molecular weight on temperature are summarized in Table I. It was observed that a higher molecular weight is obtained at 55°C compared to that obtained at 70°C . This can be due to the fact that at lower temperatures the enzyme seems to work better as a catalyst even when reaction times are longer or to the possible denaturation of the enzyme at 70°C . It is believed that, for solution polymerizations of cyclic esters such as ϵ -caprolactone in n -heptane, the thermal requirements to overcome diffusional constraints are much lower than those encountered for bulk systems.²⁰ Thus, at lower temperatures where relatively less water is “free” for chain initiation, higher molecular weight products result. Kobayashi and coworkers found large increases in percent of conversions of dodecalactone and pentadecalactone (PDL) by increasing the reaction temperature from 60 to 75°C . In their work, the reactions were conducted in bulk where diffusion constraints may be encountered. In that work lipases used were those obtained from *P. fluorescens* and lipase *Candida cylindracea* (CC). For example, using lipase CC, after a 65% PDL conversion at 75°C and 85% PDL conversion at 60°C , the product

TABLE I
Effect of Temperature in the Polymerization of ϵ -CL by *Y. lipolytica* lipase (LY)

Temperature ($^\circ\text{C}$)	Time (h)	Conversion ^a (p) %	M_n^b (Daltons)	M_n^a (Daltons)	Initial rate
50	360	14	–	600	0.0377
55	360	100	–	977	0.0136
60	360	100	620	975	0.2651
65	120	100	608	734	1.066×10^{-13}
70	264	100	540	660	0.0573

Polymerization conditions: 3 mmol ϵ -CL/100 mg of crude *Y. lipolytica* lipase in the presence of n -heptane.

^a Determined by ^1H NMR.

^b Determined by MALDI-TOF.

M_n values were 16.2×10^3 and 6.7×10^3 , respectively. Thus, by increasing the reaction temperature in viscous reaction mixtures, the mobility of the monomer and polymer components is increased and, therefore, so is the product molecular weight.²⁰

Poly(ϵ -caprolactone) characterization

In the ^1H NMR spectrum for poly(ϵ -caprolactone) synthesized *in vitro* (see Fig. 5), signals for methylene end groups *b* [$-\text{CH}_2\text{COOH}$, δ 2.35] and *q* [$-\text{CH}_2\text{OH}$, δ 3.64] are clearly seen. The other peaks in the spectrum are assigned to other methylenes of the $[-\text{CO}-(\text{CH}_2)_5-\text{O}-]$ repeating unit. Thus, the obtained asymmetric telechelic polymer has carboxylic acid $-\text{CO}_2\text{H}$ and primary hydroxyl $-\text{CH}_2\text{OH}$ end groups.

A common procedure to derivatize the PCL hydroxyl end group is based on its reaction with trifluoroacetic anhydride (TFA).²¹ The ^1H NMR spectrum for PCL (see Fig. 5) shows peaks for the hydroxylic methylene [*q*, $-\text{CH}_2\text{OH}$, δ 3.64] and the methylene adjacent to the acid carboxylic group [*b*, $-\text{CH}_2\text{CO}_2\text{H}$, overlapping]. In Figure 6 the ^1H NMR spectrum of the adduct obtained after addition of TFA to HA-PCL is shown. Formation of an ester group leads to the upfield shift for methylene *f* from δ 3.64 to 4.384 ppm [*f*, $-\text{CH}_2\text{OCOCF}_3$]. Reaction between the HA-PCL carboxylic acid end group and TFA to form anhydride [*a*, $-\text{CH}_2\text{CO}_2\text{COCF}_3$] also occurs. End-group peaks for this adduct are better resolved than those observed in the ^1H NMR spectrum of HA-PCL (see Fig. 5). Therefore, derivatization of both PCL end groups in one step can be achieved using TFA.

The ^{13}C NMR spectrum in Figure 7 also evidences the chemical nature of the HA-PCL groups. The observed peak pattern in the ^{13}C NMR spectra is similar to that reported in the literature for low mo-

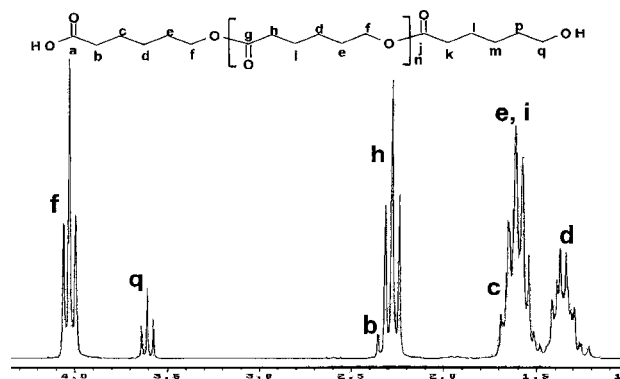


Figure 5 ^1H -NMR spectrum of poly(ϵ -CL) obtained with crude *Y. lipolytica* lipase in the presence of *n*-heptane in CDCl_3 . $R = 3$ mmol ϵ -CL/100 mg lipase. $T = 60^\circ\text{C}$. $t = 360$ h, M_n (NMR) = 975 Da.

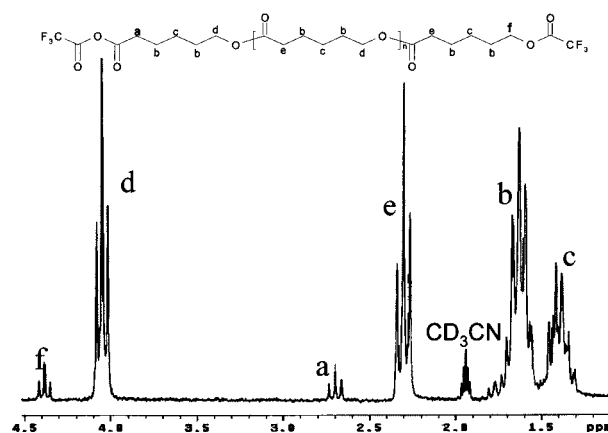


Figure 6 ^1H NMR spectrum of poly(ϵ -CL) obtained with crude *Y. lipolytica* lipase in the presence of *n*-heptane in CD_3CN , after derivatization with trifluoroacetic anhydride (TFA). $R = 3$ mmol ϵ -CL/100 mg lipase. $T = 60^\circ\text{C}$. $t = 360$ h, M_n (NMR) = 975 Da.

lecular weight HA-PCLs. In the carbonyl zone, peaks for the carboxylic acid end group [*a*, $-\text{CO}_2\text{H}$, δ 176.84] and ester carbonyl of the hydroxyl end group [*j*, $\text{OCO}-(\text{CH}_2)_5-\text{OH}$, δ 173.62] are clearly distinguished. Signals for methylene close to the hydroxyl end group [*q*, $-\text{CH}_2-\text{OH}$, δ 62.487] and carboxylic acid end group [*b*, $-\text{CH}_2-\text{COOH}$, δ 33.567] are also seen. The chemical shifts for the other methylene carbon signals (carbons *d*, *e*, *f*, *h* and *i*) are assigned based on data from literature.²¹

In Figure 8, COSY spectra for derivative obtained after treatment with TFA is shown. This spectrum provides interesting information on the end-group couplings that are not seen in the COSY spectra of PCL. Expected off-diagonal cross peaks for adjacent protons *b* and *e*, *b* and *c*, and *b* and *d* are seen in the 2-D correlation chart. Also apparent are the couplings between end-group protons *a* and *b'* (*b'* at 1.76

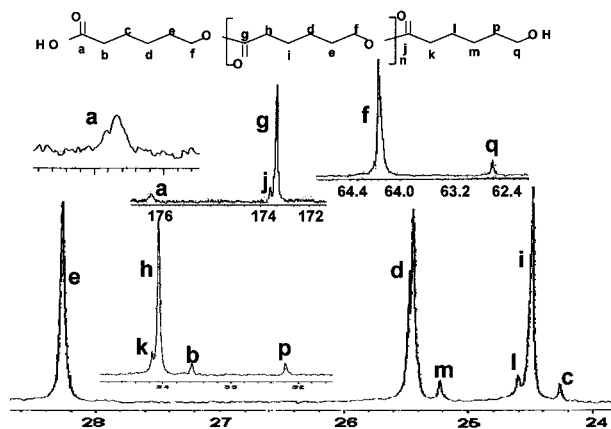


Figure 7 ^{13}C NMR spectrum of poly(ϵ -CL) obtained with crude *Y. lipolytica* lipase in the presence of *n*-heptane in CD_3Cl . $R = 3$ mmol ϵ -CL/100 mg lipase. $T = 60^\circ\text{C}$. $t = 360$ h, M_n (NMR) = 975 Da.

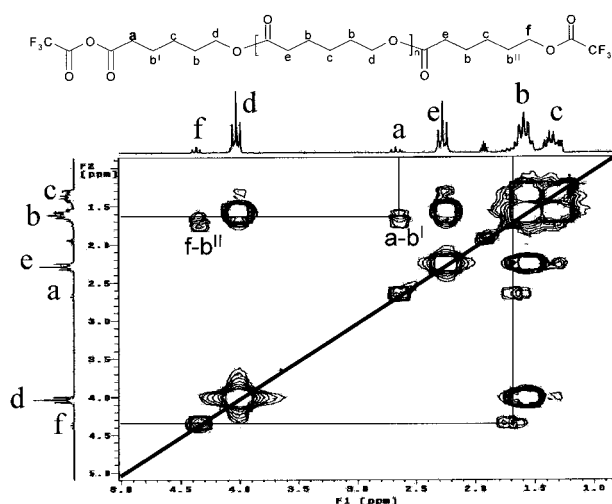


Figure 8 ^1H - ^1H homonuclear correlation (COSY) in CD_3CN for PCL ($M_n = 975$ Da) after treated with trifluoroacetic anhydride. Reaction conditions: $R = 3$ mmol ϵ -CL/100 mg *Y. lipolytica* lipase, $T = 60^\circ\text{C}$. reaction time = 360 h, in the presence of *n*-heptane.

ppm) and f and b'' (b'' at 1.66 ppm), which are effectively resolved by this technique.

In Figure 9, the MALDI-TOF mass spectrum for obtained PCL is shown. The curves profiles indicate a bimodal distribution. Four types of signals (A–D) can be distinguished in the spectrum: one due to the linear neutral polymer (A) species, other to the potassium salt (B), macrocyclic species (C) and polymer dehydrated species (D) (Scheme 2). It is well known that for broad molecular weight distributions (>1.5) the molecular weight obtained with MALDI is generally lower than the actual value. In this case, the spectrum only reflects the low molecular weight part of the distribution.

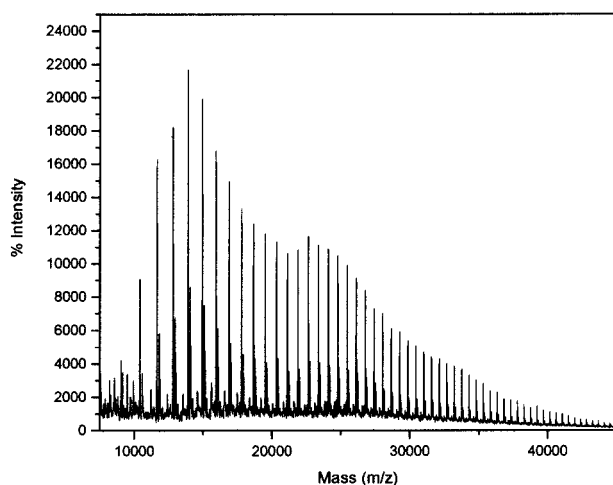
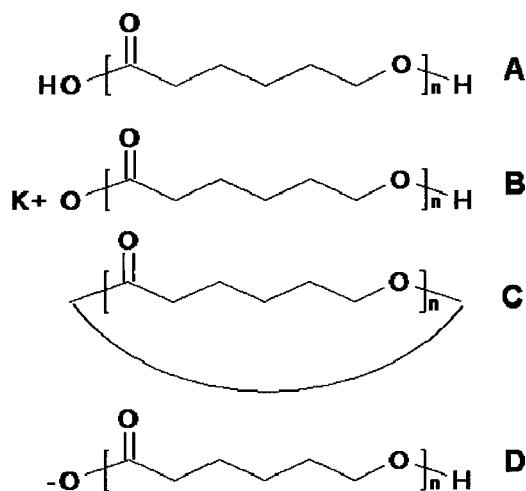


Figure 9 MALDI-TOF spectrum of poly (ϵ -caprolactone) (M_n (NMR) = 734 Da, M_n (Maldi) = 608) catalyzed with crude *Y. lipolytica* lipase in the presence of *n*-heptane. $R = 3$ mmol ϵ -CL/100 mg lipase. $T = 65^\circ\text{C}$, $t = 120$ h.



Scheme 2 Species for PCLs present in MALDI-TOF mass spectra.

In Figure 10, an expansion of the zone between 1000 and 1500 uma is shown. This region corresponds to fragments with 9–12 CL repeating units. The most intense peaks are due to HA-PCL (A) fragments, whereas the less intense peaks come from α -hydroxyl- ω -(potassium carboxylate) PCL (B) species. Species (A) are doped with sodium ions and (B) species with potassium ions.

Infrared spectroscopy has been extensively employed to determine the degree of crystallinity and to monitor the development of crystallinity in polymers. The infrared method does not yield absolute values; however, it is necessary to standardize the procedure with another technique such as X-ray diffraction. In the majority of cases, “crystalline” bands assigned in the vibrational spectra of polymers are actually associated with preferred conformations of the structural units contained in a single chain.

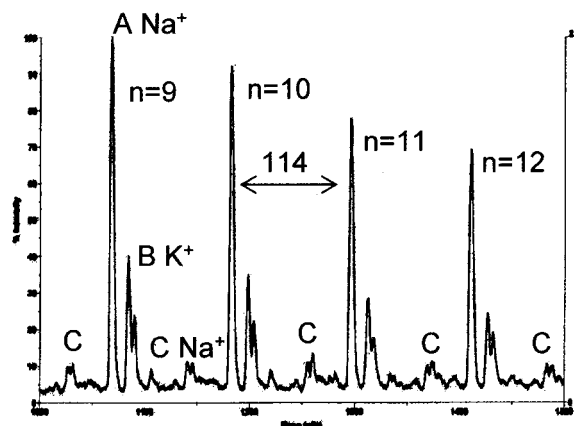


Figure 10 MALDI-TOF spectrum of poly (ϵ -caprolactone) (M_n (NMR) = 734 Da, M_n (Maldi) = 608) catalyzed with crude *Y. lipolytica* lipase in the presence of *n*-heptane. $R = 3$ mmol ϵ -CL/100 mg lipase. $T = 65^\circ\text{C}$, $t = 120$ h. Expanded view for the 1000–1500 fragments.

As PCL is a semicrystalline polymer in the solid state, the infrared spectrum consists of contributions from both the crystalline and amorphous phases. It has been demonstrated that for polymers with relatively large repeating units, the crystalline component of the infrared spectrum of the polymer can be recognized and even readily separated from the amorphous component by using digital subtraction techniques.²² Effect of polymerization temperature in the final polymer morphology can be detected using FTIR spectroscopy.²³

Figure 11 shows the ATR FTIR spectra (carbonyl zone) for PCL obtained by enzymatic polymerization with *Y. lipolytica* lipase at different temperatures. The observed peak patterns reflect differences in polymer morphology. In semicrystalline PCL, carbonyl stretching frequency (C=O) is observed at 1724 and 1737 cm^{-1} for the crystalline and amorphous phases, respectively. The amorphous band is characteristically broader than that for the crystalline component, reflecting an increase in conformational freedom.²⁴ Other authors have reported that a peak for hydrogen-bonded component in PCL can be observed at 1708 cm^{-1} .²⁵ As can be observed in Figure 11, peak pattern for each sample is different, as morphology of the three samples is not the same. In all spectra, a peak at 1722 cm^{-1} for the crystalline component is present. The other assigned peaks (corresponding to the amorphous phase) were resolved by recording the minima of the second derivative spectra. Peaks shapes for PCLs obtained at 60 and 65°C are alike, being that for polyester obtained at 70°C broader. Because of the lower molecular weight, it is expected that the content of hydroxyl groups for this sample be higher, and this in turns leads to the formation of a considerable amount of hydrogen-bonded species.

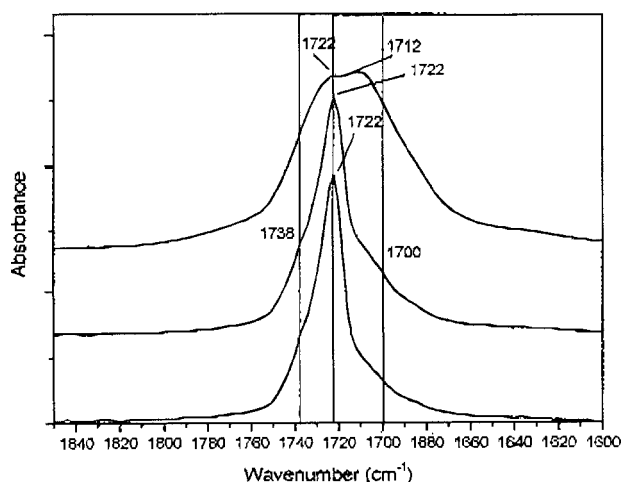


Figure 11 ATR FTIR spectra (carbonyl zone) for PCL obtained by enzymatic polymerization with *Y. lipolytica* lipase in the presence of heptane. $R = 3 \text{ mmol } \epsilon\text{-CL}/100 \text{ mg lipase}$.

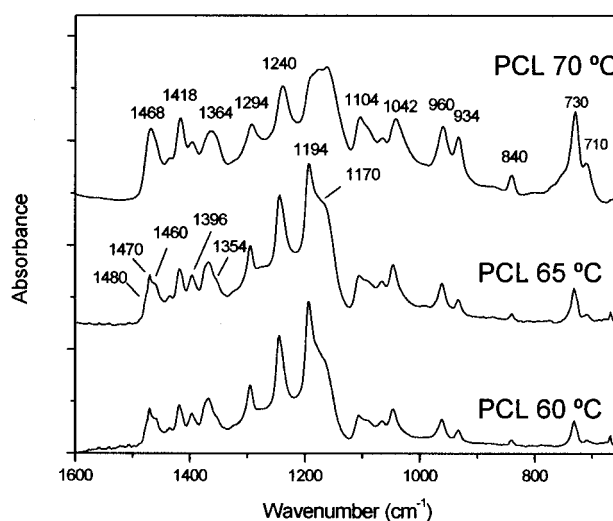


Figure 12 ATR FTIR spectra ($1600\text{--}700 \text{ cm}^{-1}$ region) for PCL obtained by enzymatic polymerization with *Y. lipolytica* lipase in the presence of *n*-heptane. $R = 3 \text{ mmol } \epsilon\text{-CL}/100 \text{ mg lipase}$.

Peak patterns (see Fig. 12) in the $700\text{--}1600 \text{ cm}^{-1}$ zone also reflects differences in morphology. In this zone, relatively sharp, well-defined bands are seen. The bands that appear between 1110 and 1300 cm^{-1} are coupled modes variously associated with C—C—H and O—C—H bending, and C—C and C—O stretching vibrations. The main differences are observed for peaks at 1470 ($\delta_{\text{as}} \text{CH}_3$), 1364 ($\delta_{\text{s}} \text{CH}_3$), 1194 ($\nu \text{ C—O}$), 1170 , 730 , and 710 cm^{-1} ($\rho \text{ CH}_2$). In particular, the latter signals corresponding to methylene rocking vibrations ($\rho \text{ CH}_2$) are more intense for samples with lower molecular weight. It is

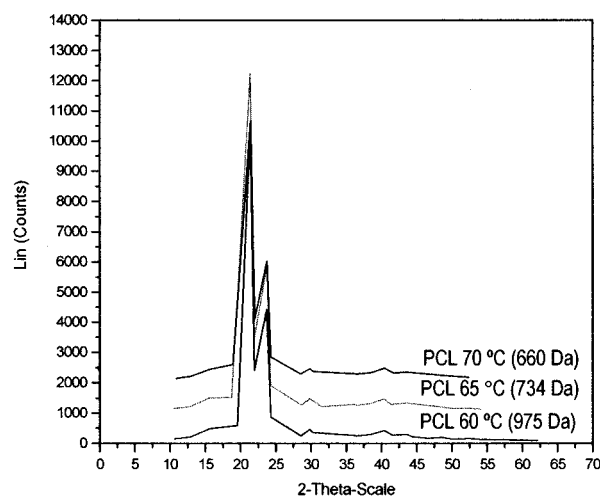


Figure 13 Wide angle X-ray scattering (WAXS) spectra for PCL obtained by enzymatic polymerization with *Y. lipolytica* lipase in the presence of *n*-heptane. $R = 3 \text{ mmol } \epsilon\text{-CL}/100 \text{ mg lipase}$.

TABLE II
Materials, Molecular Weights, and
Degrees of Crystallinity

Material	M_n^a (Daltons)	M_n^b (Daltons)	Degree of crystallinity ^c (%)
PCL60	620	977	78.6
PCL65	608	734	76 \pm 1
PCL70	540	660	54 \pm 1

Polymerization conditions: 3 mmol ϵ -CL/100 mg of crude *Y. lipolytica* lipase in the presence of *n*-heptane.

^a Obtained by MALDI-TOF.

^b Obtained by ¹H NMR.

^c Obtained by DSC.

reported for polyethylene that the transition moments for these methylenes are parallel to the *a*-crystal axis, and the signal at 710 cm⁻¹ is related with a monoclinic structure.²⁶ This feature indicates the existence of a crystalline phase that is more abundant in the sample obtained at higher temperature.

PCL crystallinity for obtained samples was also studied by WAXS. Figure 13 shows the diffraction profiles for PCLs. In the diffractograms for PCL, an intense peak at $\theta = 10.6^\circ$ and two smaller ones at 10.9 and 11.8 $^\circ$ are generally seen. Small differences can be observed between samples, but amorphous halo is more important for PCL with lower molecular weight. A lower degree of crystallinity was recorded for this sample by DSC (see Table II).

Amorphous and crystalline components in polymer can be separated based on mobility by solid-state

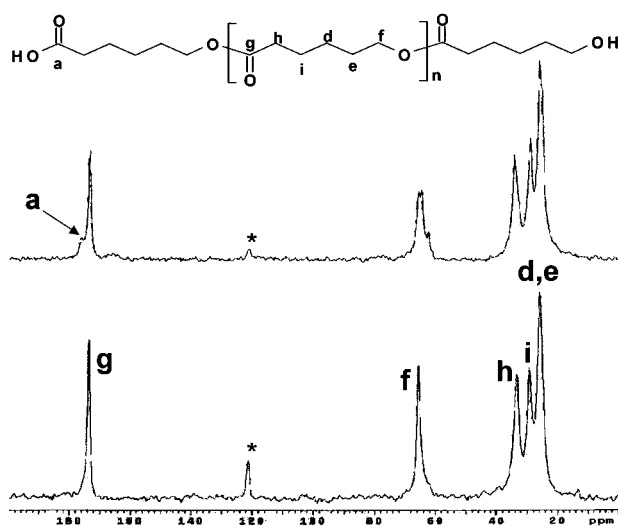


Figure 14 Solid-state ¹³C-NMR (75.47 MHz) spectrum for poly (ϵ -CL) obtained with crude *Y. lipolytica* lipase in the presence of *n*-heptane. $R = 3$ mmol ϵ -CL/100 mg lipase. $T = 60^\circ\text{C}$. $t = 360$ h, M_n (NMR) = 975 Da. (a) CPMAS spectrum, contact time 1 ms, repetition time 3 s; (b) MAS spectrum with a repetition time of 20 s. Spinning sidebands are indicated by an asterisk.

NMR. Efficiency of cross-polarization in the crystalline region is in general larger than in the noncrystalline regions.²⁷ CP-MAS and MAS ¹³C NMR spectra for PCL obtained at 60 $^\circ\text{C}$ are shown in Figure 13. Peak patterns observed in the CP-MAS spectra for all PCLs are similar to those reported in the literature²⁸ However, MAS spectra show important differences, in particular for signals due to carbonyl and to the methylene carbon adjacent to oxygen.

In the carbonyl zone (MAS spectrum), a sharp peak due to carboxyl (173.7 ppm) separated from a shoulder at 176 ppm (due to a end-group carboxylic acid functionality, see arrow in (Fig. 14) can be seen in the MAS spectra. Peak for carboxylic acid is not clearly observed in the CP-MAS spectra. The most

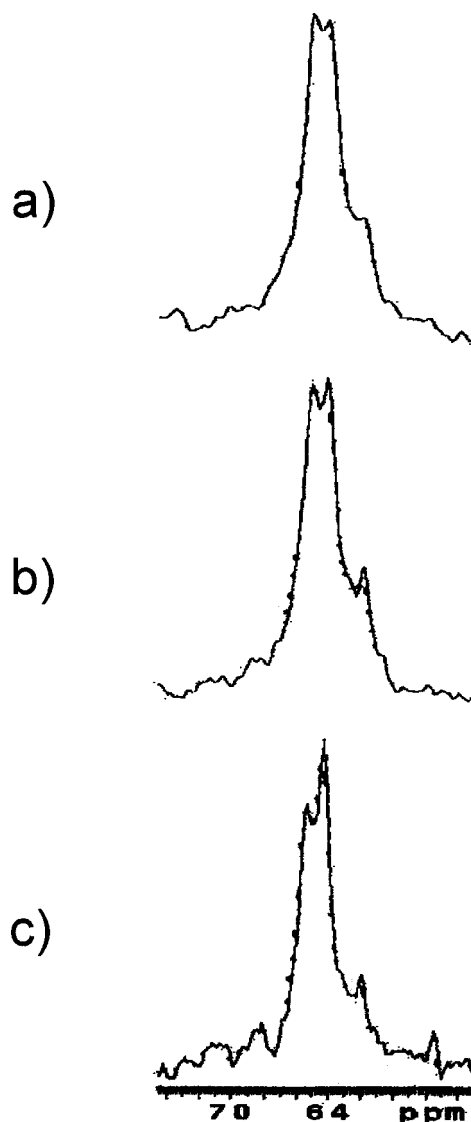


Figure 15 Solid-state MAS ¹³C-NMR (75.47 MHz) spectrum for poly (ϵ -CL) obtained with crude *Y. lipolytica* lipase in the presence of *n*-heptane. $R = 3$ mmol ϵ -CL/100 mg lipase, at different temperatures, (a) $T = 60^\circ\text{C}$ (bottom), (b) $T = 65^\circ\text{C}$ (middle) and (c) $T = 70^\circ\text{C}$ (top).

notorious differences are seen in the methylene linked to oxygen zone (carbon *f*, see Fig. 15). These differences indicate the coexistence of various types of phases, which are formed during crystallization. Occurrence of cocrystallization is rare in Polymer Science²⁹ and there are not previous reports on this phenomena in PCLs.

Figure 16 shows the DSC curves for PCL during the first heating. Biphasic morphology is apparent. In the second heating (Fig. 17), the biphasic pattern is better resolved. Degree of crystallinity obtained by DSC is shown in Table IV. Observation of two peaks indicates the existence of a multiphase morphology, but more experiments are necessary to obtain information on the phases present in the samples.

CONCLUSIONS

Yarrowia lipolytica lipase production is favored when wheat flour and used commercial oil is used instead of olive oil, with an incubation time of 16.5 h at 29°C and 250 rpm. In this way, the preculture step can be avoided. Lipase obtained from *Y. lipolytica* is homogeneous and has higher purity than that obtained by traditional methods.

Solid polyesters with relatively high degree of crystallinity, number-average molecular weights M_n in the range of 660–975 Da and melting points in the range of 50.7–59.5°C (observed by DSC) were obtained. Higher polymerization temperatures lead to the formation of polymers with lower molecular weights, melting points and degree of crystallinity (WAXS). MALDI-TOF spectra show a bimodal molecular weight distribution. In the DSC thermograms,

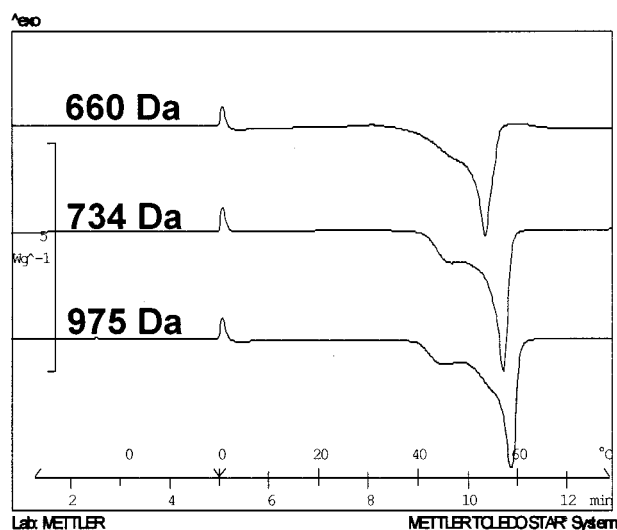


Figure 16 DSC first heating curves (20°C/min) of poly (ϵ -CL) obtained with crude *Y. lipolytica* lipase in the presence of *n*-heptane. $R = 3$ mmol ϵ -CL/100 mg lipase.

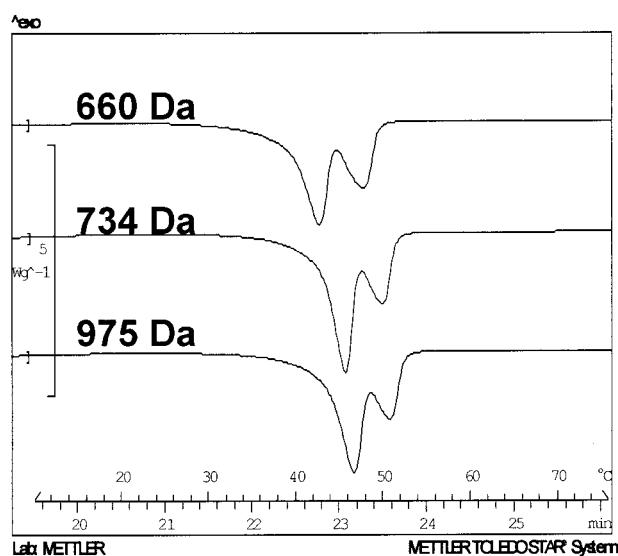


Figure 17 DSC second heating curves (20°C/min) of poly (ϵ -CL) obtained with crude *Y. lipolytica* lipase in the presence of *n*-heptane. $R = 3$ mmol ϵ -CL/100 mg lipase.

evidence of multiphase morphology in the obtained polyesters is served.

By FTIR, peaks associated with the different crystalline phases present in the polymer can be identified.

As expected from the current accepted mechanism for ROP of CL by lipases, final polymers are asymmetric telechelic α -hydroxy- ω -carboxylic acid poly (ϵ -caprolactones), as determined by proton and carbon-13 NMR.

We acknowledge the comments of the reviewer. We are indebted to Ángel Marcos-Fernández and Rosa Lebrón-Aguilar (CSIC, Madrid España) for MALDI-TOF spectra and useful discussion, and Leticia Baños (Instituto de Investigaciones en Materiales, UNAM) for WAXS spectra.

References

- Pandey, A.; Sailas, B.; Soccol, R. C.; Nigam, P.; Krieger, N.; Soccol, V. T. *Biotechnol Appl Biochem* 1999, 29, 119.
- Sharma, R.; Chisti, Y.; Banerjee, U. C. *Biotechnol Adv* 2001, 19, 627.
- Martinelle, M.; Holmquist, M.; Hult, K. *Biochim Biophys Acta* 1995, 1258, 272.
- Beckerich, J. M.; Boisramé-Baudevin, A.; Gaillardin, C. *Int Microbiol* 1998, 1, 123.
- Barth, G.; Gaillardin, C. In *Nonconventional Yeasts in Biotechnology: A Handbook*; Wolf, K., Ed.; Springer: Berlin, Heidelberg, 1996; p 313.
- Barth, G.; Gaillardin, C. *FEMS Microbiol Rev* 1997, 19, 219.
- Knani, D.; Gutman, A. L.; Kohn, D. H. *J Polym Sci Part A: Polym Chem* 1993, 31, 1221.
- Uyama, H.; Kobayashi, S. *Chem Lett* 1993, 1149.
- Kobayashi, S.; Uyama, H.; Kimura, S. *Chem Rev* 2001, 101, 3793.
- Kobayashi, S.; Uyama, H. *Curr Org Chem* 2002, 6, 209.
- Varma, I. K.; Albertsson, A. C.; Rajkhowa, R.; Srivastava, R. K. *Prog Polym Sci* 2005, 30, 949.

12. Bartniki-García, S.; Nickerson, W. J. *J Bacteriol* 1962, 84, 829.
13. Bradford, M. M. *Anal Biochem* 1976, 72, 248.
14. Destain, J.; Roblain, D.; Thonart, P. *Biotechnol Lett* 1997, 19, 105.
15. Imanaka, T.; Muto, K.; Ohkuma, S.; Takano, T. *Biochem et Biophys Elsevier Acta* 1981, 665, 322.
16. Laemmli, U. K. *Nature* 1970, 227, 680.
17. Merrill, C. R. *Meth Enzymol* 1990, 182, 477.
18. Koenig, M. F.; Huang, S. *J Polym* 1995, 36, 1877.
19. Segura, R. L.; Betancor, L.; Palomo, J. M.; Hidalgo, A.; Fernandez-Lorente, G.; Terreni, M.; Mateo, C.; Cortes, A.; Fernandez-Lafuente, R.; Guisan, J. M. *Enzyme Microb Technol* 2006, 29, 817.
20. Gross, R. A.; Kumar, A.; Kalra, B. *Chem Rev* 2001, 2097, 101.
21. Baez, J. E.; Martínez-Richa, A.; Marcos-Fernández, A.; *Macromolecules* 2005, 38 1599.
22. Koenig, J. L.; *Spectroscopy of Polymers*, 2nd ed.; Elsevier: New York, 1999.
23. Coleman, M. M.; Tabb, D. L.; Koenig, J. L. *Polym Lett* 1974, 2, 12577.
24. Coleman, M. M.; Zarian, J. *J Polym Sci: Polym Phys Ed* 1979, 17, 837.
25. Coleman, M. M.; Painter, P. C. *Appl Spectr Rev* 1984, 20, 255.
26. Holland-Morritz, K.; van Werden, K. *Makromol Chem* 1981, 182, 651.
27. Tonelli, A. E. In *NMR Spectroscopy of Polymers*; Ibbet, R. N., Ed.; Blackie Academic: London, 1993; p 161.
28. Mathias, L. L.; Colleti, R. F.; Halley, R. J.; Jarrett, W. L.; Johnson, C. G.; Powell, D. G.; Warren, S. C. *Solid-State NMR Polymer Spectra*, Collected Volume 1; MRD Polymer Press: Hattiesburg, MS; p 89.
29. Inoue, Y. In *Solid-State NMR of Polymers. Studies in Physical and Theoretical Chemistry (Solid State NMR of Polymers, Vol. 84)*; Ando, I.; Asakura, T., Eds.; Elsevier, 1988; pp 771–817.